Rapid Communications

Identification of nickel-vacancy defects by combining experimental and *ab initio* simulated photocurrent spectra

E. Londero,[1] E. Bourgeois,[2,3] M. Nesladek,[2,3] and A. Gali[1,4]

[1]*Wigner Research Center for Physics and Optics, Hungarian Academy of Sciences, P.O. Box 49, H-1525 Budapest, Hungary*

[2]*IMOMEC Division, IMEC, Wetenschapspark 1, B-3590 Diepenbeek, Belgium*

[3]*Institute for Materials Research (IMO), Hasselt University, Wetenschapspark 1, B-3590 Diepenbeek, Belgium*

[4]*Department of Atomic Physics, Budapest University of Technology and Economics, Budafokiút 8., H-1111 Budapest, Hungary*

(Received 10 October 2017; published 12 June 2018)

There is a continuous search for solid state spin qubits operating at room temperature with excitation in the infrared communication bandwidth. Recently, we have introduced the photoelectric detection of magnetic resonance (PDMR) to read the electron spin state of nitrogen-vacancy (NV) centers in diamond, a technique which is promising for applications in quantum information technology. By measuring the photoionization spectra on a diamond crystal, we found two ionization thresholds of unknown origin. On the same sample we also observed absorption and photoluminescence signatures that were identified in the literature as Ni-associated defects. We performed *ab initio* calculations of the photoionization cross section of the nickel split-vacancy complex (NiV) and N-related defects in their relevant charge states and fitted the concentration of these defects to the measured photocurrent spectrum, which led to a surprising match between experimental and calculated spectra. This study enabled us to identify the two unknown ionization thresholds with the two acceptor levels of NiV. Because the excitation of NiV is in the infrared, the photocurrent detected from the paramagnetic NiV color centers is a promising way towards the design of electrically readout qubits.

DOI: 10.1103/PhysRevB.97.241202

Diamond is rich in point defects that are able to change the optical and electrical properties of the host material, often called color centers [1]. One of the prominent color centers in diamond is the nitrogen-vacancy (NV) defect. In particular, the negatively charged NV (NV^-) color center acts as a solid state quantum bit [2,3] which can be employed in diverse nanoscale sensing [4–9] and quantum communication applications [10–12]. These quantum applications of the NV center are based on the long spin coherence time of the NV center [2,13] and the optical readout and initialization of the spin state [14]. Recently, the spin state of NV^- has been detected by photoelectric detection of magnetic resonance (PDMR) [15]. In this scheme, the electron spin state is initialized optically, then illumination is applied to promote the electron to the conduction band, and finally the resulting photocurrent is detected. It has been found that the photoionization is spin selective, that is the base of PDMR readout of the spin state [15]. Recent advances in the enhancement of the PDMR contrast for readout [16–18] pave the way towards the detection of single NV center spins. The detected electron rate of PDMR is significantly higher than the photon rate of optically detected magnetic resonance [15]. In recent experiments, by applying dual beam photoexcitation [17], we were able to increase further the photoelectric detection rate of NV's. In our efforts in studying the mechanism of photoionization of the NV defect [17] and measuring the photocurrent response of the diamond sample in a wide spectral range, two photocurrent bands of unknown origin appeared in the near-infrared (NIR) range at about 1.2 and 1.9 eV. The identification of these ionization bands is of high importance, at least for two reasons: (i) Photoresponsive defects give an unwanted background in the PDMR spectrum of NV^-, reducing the PDMR contrast, and therefore their identification guides the fabrication of diamond materials to avoid their presence; (ii) these defects, which can be certainly photoionized, might turn out to be advantageous for the electrical detection of spin states as an alternative to the NV center if they have favorable magneto-optical properties. Specifically for the electrical readout of spin centers, strong optical radiative transitions are not *a priori* necessary, and the as yet unidentified defects may outperform the NV quantum bits in diamond. Qubits enabling initialization in the near-IR part of the spectrum are specifically interesting for quantum information applications.

In this Rapid Communication, we apply density functional theory (DFT) to identify the origin of the photocurrent bands detected on an irradiated and annealed nitrogen-rich diamond, by comparing the calculated and experimental photocurrent spectra. We find that the bands originate from the two acceptor levels of the nickel split-vacancy complex, which we label NiV here. We propose that since the NiV complex can potentially act as a solid quantum state bit, it could be a good candidate for future PDMR studies in the NIR region.

The experimental photocurrent spectra were taken from a type-Ib high-pressure high-temperature (HPHT) diamond plate that was irradiated by protons with an energy of 6.5 MeV and a dose of 1.13×10^{16} cm^{-2} and subsequently annealed for 1 h at 900 °C under argon atmosphere. After this treatment, the sample was cleaned and oxidized. For photocurrent spectroscopy measurements, the sample was equipped with coplanar electrodes (interelectrode distance 100 μm). A

monochromatic light (1–300 μW depending on the wavelength) produced using a halogen lamp associated with a monochromator was focused onto the sample. The free charge carriers induced by photoionization of the defects in the diamond crystal were directed toward electrodes by applying a dc electric field of 5×10^4 V cm^{-1}. The resulting photocurrent was preamplified, measured by lock-in amplification, and normalized to the flux of incoming photons. The total photocurrent spectrum contains the contributions resulting from the ionization of individual defects at a given concentration. The continuous-wave photoexcitation leads to a steady state balance between the charge states of the defects that is different from the thermal equilibrium. As a consequence, the observed concentration of a defect in a given charge state may change when the conditions of illumination are varied. To better identify the origin of the defects responsible for photoionization bands, two methods were applied in the photocurrent spectroscopy experiments. In the first case (method 1), no blue bias light illumination was applied, whereas in the second case (method 2), a blue bias illumination (parameters: 2.4–3 eV excitation energy and 1.8 mW power) was used. The blue bias light allows us to manipulate the occupation of deep defects, which is particularly useful for selectively promoting (or excluding) the photoionization of specific defects.

On the spectrum recorded without blue bias light (method 1), a broad ionization band with an onset around 2.7 eV is observed [see Fig. 1(a)]. Our previous work has shown that this feature resulted from a combination of the ionization bands of substitutional nitrogen (N_s^0), NV^0 and NV^- (see Ref. [17]). An additional band with an onset around 1.9 eV can also be distinguished. In the presence of a blue bias light (method 2), the photocurrent associated with the 1.9-eV ionization band increases and a new photocurrent band with a threshold around 1.2 eV emerges [see the red curve in Fig. 1(a)]. We note that red light illumination (1.75–1.95 eV excitation energy and 1.5 mW power) did not produce the same effects.

To identify the defects potentially responsible for the unidentified photocurrent bands with an onset at 1.2 and 1.9 eV, the sample was further characterized by photoluminescence (PL), Fourier transformed infrared absorption (FTIR), and optical absorption spectroscopy [see Figs. 1(b)–1(d)]. The concentration of NV^- was estimated to be $[NV^-] \sim 34$ ppm, by comparing the PL intensity measured in the confocal mode to that measured using the same objective on a reference high-pressure high-temperature (HPHT) sample with a calibrated NV^- concentration. The concentration of NV^0 centers is evaluated by comparing the PL spectrum obtained under low continuous-wave green light excitation to the spectra obtained on single NV^- and NV^0 (see Ref. [20]), which resulted in $[NV^0] \sim 1.1$ ppm. The concentration of N_s^0 was estimated from the absorption coefficient at 1130 cm^{-1}, determined by FTIR absorption spectroscopy [21], which yielded $[N_s^0] \sim 220 \pm 20$ ppm. The absorption peak of N_s^+ at 1332 cm^{-1} [22] is not detected, indicating that in this sample the N_s defect is in a large majority in its neutral state. These data are summarized as "dark expt." in Table II. Beside the signatures of NV^0 (photoluminescence observed below 639 nm) and NV^- defects [zero phonon line (ZPL) at 639 nm and associated phonon sidebands at higher wavelengths], a broad peak is observed in the PL spectrum at a wavelength of 678 nm (1.83 eV).

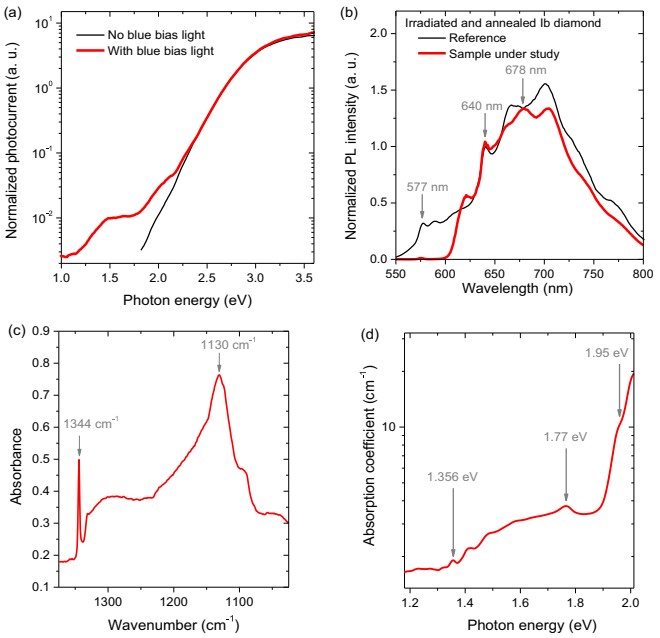

FIG. 1. (a) Photocurrent spectra measured on irradiated and annealed type-Ib diamond without (method 1) and with (method 2) blue bias illumination. (b) Photoluminescence (PL) spectra (excitation: 532 nm, 1.6 mW). The PL peak at 678 nm, observed in the spectrum of the sample under study (red curve) and attributed to a Ni-related defect, was not detected in the spectrum of a reference irradiated and annealed type-Ib diamond (shown for comparison, black curve). (c) FTIR spectrum. The absorption peaks of N_s^0 at 1344 and 1130 cm^{-1} can be observed. (d) Optical absorption coefficient in the UV-visible range, measured at 77 K. The ZPL of NV^- appears at 1.95 eV. The absorption peak detected at 1.77 eV, already reported on irradiated type-Ib diamond, has been attributed to an interstitial defect [19]. The ZPL at 1.356 eV and associated phonon replica at higher energies have been observed in diamond containing both N and Ni [1,19].

This peak is associated with a nickel defect [23–28]. The photoluminescence emission rate for this defect is unknown, therefore the concentration of the Ni-related defects cannot be determined from these data. More evidence for the presence of nickel is the ZPL at 1.356 eV and the associated phonon replica observed in the UV-visible absorption spectrum which were reported for synthetic diamonds containing Ni and N (see Refs. [1,29]).

The thresholds of the two unidentified ionization bands observed at 1.2 and 1.9 eV in photocurrent spectra closely resemble our calculation of the first and second acceptor levels of the NiV defect at $E_V + 1.22$ eV and $+1.90$ eV [28], respectively, where E_V is the valence band maximum. Although other Ni-related defects may exist in the sample, only the NiV^0 and NiV^- show photoionization bands at $\approx$1.2 and 1.9 eV, respectively. Therefore, our working model is that the ionizations of NiV^0 and NiV^- are responsible for these features. To verify this hypothesis, we used DFT calculations to determine the photocurrent spectra obtained considering ionization of the nitrogen- and nickel-associated defects present in the sample, and compared the calculated spectra obtained in this way to the measured spectra.

To calculate the energy dependence of defects' ionization cross sections, we apply *ab initio* Kohn-Sham DFT calculations. In the photoionization process, an electron is excited from an in-gap defect level to the conduction band (CB) or from the valence band (VB) to an in-gap defect level. The photoionization probability is then directly proportional to the absorption cross section that depends on the imaginary part of the dielectric function related to the transition between the initial ground state and the final excited state. This process can be well approximated by the transition of a single electron from/to the in-gap defect level to/from the band edges, thus the imaginary part of the dielectric function can be calculated between the corresponding Kohn-Sham states and levels. Our tasks are therefore to calculate (a) the excitation energies and (b) the corresponding imaginary part of the dielectric function.

(a) In the optical excitation process, the atoms may change their geometry with respect to their ground state. We consider this effect within the Franck-Condon approximation, and calculate the lowest-energy excitation that corresponds to the pure electronic transition, i.e., the ZPL energy. This is calculated with the so-called Δ-self-consistent-field (ΔSCF) DFT approach as was demonstrated for the NV center [30]. Here, it is critical to apply a DFT functional which is able to reproduce the band gap of diamond and the in-gap defect levels. According to our previous studies [30,31], this can be achieved by a range-separated and screened hybrid density functional [functional of Heyd-Scuseria-Ernzerhof (HSE06)] [32,33]. Here, we particularly calculated the ZPL energies only for the band edges explicitly, and we assumed that the larger excitation energies follow the calculated bands with respect to the band edges. We note that an alternative is to simply calculate the adiabatic charge transition level. In this case, the exciton binding energy is neglected. As shown below, the exciton binding energy can be indeed neglected.

(b) In the Franck-Condon approximation, the imaginary part of the dielectric function for the ZPL transition is the same as it is for the corresponding phonon sidebands. Thus, the imaginary part of the dielectric function can be calculated at the ground-state geometry. We note that optical transitions to the bands require an accurate calculation of the electron density of states. In practice, this implies involving many k points in the Brillouin zone. However, an HSE06 calculation with many k points is computationally prohibitive in a large supercell embedding the defect. Thus, we applied the semilocal Perdew-Burke-Ernzerhof (PBE) functional [34] since PBE and HSE06 functionals produce very similar Kohn-Sham wave functions for calculating the optical transition dipole moments.

The defect was modeled in a 512-atom diamond supercell. We applied the Γ point for the geometry optimization of the defects. We note that the Γ point in this supercell folds the k point of the conduction band minimum. The geometry is converged when the forces acting on the atoms are lower than 0.02 eV/Å. We calculate the DFT charge and spin densities of the systems by the VASP code [35,36], using the projector augmented-wave (PAW) formalism [37]. Standard PAW potentials are chosen for the N and C ions and Ni 3d electrons are treated as valence electrons. A plane-wave basis set is utilized to expand the wave function of the valence electrons. The energy cutoff for the expansion of the plane waves is set to 370 eV. The total energy of the charged supercell was corrected both in the ground and excited states to cancel the finite-size errors [38]. We found that $6 \times 6 \times 6$ Γ-centered k-point sampling of the Brillouin zone produces converged electron density states in the conduction bands and the valence bands. We applied this k-point set for defects possessing C_{3v} symmetry in the calculation of the imaginary part of the dielectric function. We calculated this property of defects with C_{1h} symmetry only within $4 \times 4 \times 4$ Γ-centered k-point sampling of the Brillouin zone, yielding also converged results in the energy region of interest. The calculated optical absorption functions were finally constructed by following the recipe of (a) and (b) with an additional Gaussian smearing of 0.2 eV to simulate the vibration effects at room temperature.

TABLE I. Relevant ionization energies used in the construction of the photocurrent spectrum that are given in eV units. The NV^+ is shown for the sake of completeness but it does not appear in the photocurrent spectrum. For NV and NiV defects, the ionization energies are determined from HSE06 DFT calculations, whereas the experimental one is applied for N_s^0. UV means ultraviolet photoexcitation energy that is outside the range of our experiments.

Defect	(+) → (0)	(0) → (+)	(0) → (−)	(−) → (0)	(−) → (2−)
NV	0.99	UV	2.74	2.78	
N_s	UV	2.20			
NiV			1.22	UV	1.90

To reconstruct the photocurrent spectra, the calculation was performed for all the major defects present in the sample in their relevant charge states. We first discuss photophysics of NV and N_s defects in detail (see Table I). For N_s, the neutral and positive charge states are considered, whereas neutral, negative, and positive charge states are taken into account for NV (see Ref. [39]). We find that the exciton binding energy of these defects (see Supplemental Material [40]) can be neglected at room temperature with respect to the broadening effects due to vibrations in the photocurrent spectrum.

The following conclusions can be drawn for the NV defect from these results: (i) The $NV^- \rightarrow NV^0$ and $NV^0 \rightarrow NV^-$ transition energies almost coincide at ∼2.76 eV, thus the individual ionization bands cannot be resolved in the room-temperature photocurrent spectrum; (ii) the estimated energy of the intra-defect-level optical transition (see Ref. [40]) is larger than the band-edge excitation energy for NV^+, thus NV^+ might show up as a weak absorption at around 1 eV; (iii) NV^0 can be ionized to NV^+ only by ultraviolet excitation (≈4.2 eV), but the $NV^0 \rightarrow NV^-$ transition is active in this energy region. We conclude that photoexcitation in the visible range induces cycles between NV^- and NV^0, and transitions to NV^+ do not occur. In addition, the calculated $NV^+ \rightarrow NV^0$ transition energy is lower by 0.2 eV than the 1.2-eV ionization band in the photocurrent spectrum that is above the uncertainty of our method. We conclude that NV^+ does not show up in the photocurrent spectrum.

The photoionization of N_s^0 requires a short discussion. This defect has a giant reorganization energy (1.37 eV; see Ref. [40]) of the ions upon ionization. The reason behind this phenomenon is that N_s^0 is a Jahn-Teller unstable system in T_d symmetry and it strongly reconstructs to C_{3v} symmetry.

Thus, the ionization cross section is very minor at the ZPL energy but much stronger with the participation of phonons that drive the atoms from the high T_d symmetry to the reconstructed C_{3v} symmetry. This effect was already discussed in previous studies [41,42]. In experimental studies [41,42], the photoionization threshold of N_s was found at ≈2.2 eV by using the Inkson's formula [43] for the photoionization cross section of deep level defects. This finding explains the long-standing unresolved discrepancy between the thermal ionization of N_s^0, i.e., its energy in the band gap at thermal equilibrium (1.7 eV below the CB), and its photoionization energy (2.2 eV). However, it is beyond the scope of this study to directly involve phonons in the calculated photocurrent spectrum. We rather used the experimental value of 2.2 eV for the ionization threshold of N_s^0 instead of the calculated ZPL energy.

The neutral and the negative charge states of the NiV color center were already studied in a previous work by means of our *ab initio* method [28]. We note that the split-vacancy configuration of this defect constitutes a high D_{3d} symmetry where Ni sits at the inversion center of diamond near two adjacent vacancies, i.e., in divacancy. This defect may be labeled as V-Ni-V, in order to note the interstitial position of the Ni impurity atom. However, quantum optic groups often label the split-vacancy complexes of the X impurity as the XV color center, e.g., group-IV–vacancy complexes. Thus, we decided to use this nomenclature for Ni, too. The detailed discussion of the electronic structure of the defect can be found in Ref. [28]: Briefly, a doubly degenerate e_u level appears in the gap which is occupied by two electrons with parallel spins in the neutral charge state that establishes an $S = 1$ ground state. This can be further occupied by one or two electrons that leads to single and double acceptor states and levels with $S = 1/2$ and $S = 0$ spin states, respectively (see Table I).

To reconstruct the photocurrent spectrum measured following method 1 [no blue bias light; see Fig. 1(a)], we assumed that all N_s centers are in the neutral charge state, thus we fixed the concentration of N_s^0 at the experimental value of 200 ppm. We then varied the concentrations of NV^- and NV^0 (threshold around 2.76 eV) and NiV^- (threshold around 1.9 eV), in order to fit to the experimental photocurrent spectrum (dotted red line in Fig. 2). We note that the calculated ionization cross section in a wide region of energies is significantly larger for NV^0 than that for NV^-. This explains why the green photoexcitation of individual NV defects can stabilize NV^- over NV^0. From the fit we find the calculated [NV^-] and [NV^0] at 31.4 and 1.0 ppm, respectively, i.e., close to the values of ≈34 and ≈1.1 ppm, respectively, deduced from experiments (see Table II). The fitted concentration of NiV^- is about 1.2 ppm. It is likely that these Ni defects reside in the region of diamond with neutral NV centers where the quasi-Fermi level is lower than that in the other regions of diamond.

To reconstruct the photocurrent spectrum obtained under blue bias illumination [method 2; see Fig. 1(a)], we associate the ionization band with a threshold around 1.2 eV to the ionization of NiV^0 (see the red dotted curve in Fig. 3). Indeed, the results of our simulation imply that blue illumination produces holes that yield more NV^0, NiV^-, and NiV^0, at the expense of less N_s^0 and NV^-. The calculated concentration of NiV^0 is 0.14 ppm under blue bias illumination (see Table II), whereas that of NiV^- increased substantially compared to that

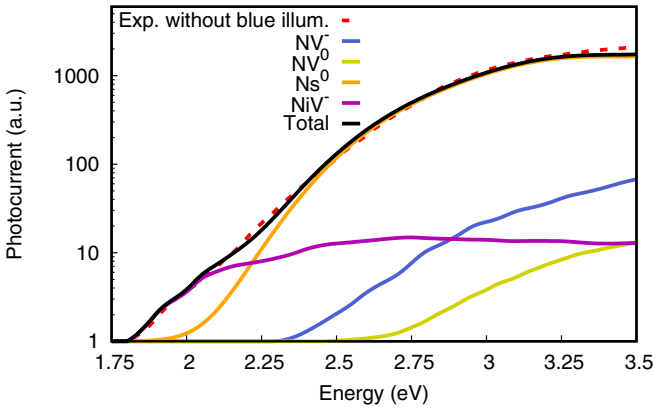

FIG. 2. The photocurrent spectrum measured on our sample in the absence of blue bias light (method 1) is fitted to the concentrations of NV^-, NV^0, and NiV^- defects using *ab initio* calculated ionization cross sections. The concentration of N_s was fixed at 200 ppm. The defect concentrations resulting from the fit are listed in Table II, in the line entitled "no blue."

obtained by fitting the spectrum measured in the absence of bias light. We attribute this effect to the fact that NiV^{2-} defects capture holes and are converted to NiV^- and, to a lesser extent, NiV^0 under blue illumination. The results are summarized in Table II.

Our combined experimental and atomistic simulation study identified the NiV defect in an irradiated and annealed type-Ib diamond sample. We note that an absorption center was found at 1.22 eV in Ni contaminated diamond [44] that was correlated with the NOL1/NIRIM5 electron paramagnetic resonance (EPR) spectrum [45,46]. Based on our modeling, the 1.22-eV absorption peak can be well explained by the optical transition from the valence band edges to the empty defect level in the spin minority channel. The NOL1/NIRIM5 EPR center possesses a giant zero-field splitting of $D = -171$ GHz, and a relatively large anisotropy in the g-tensor, $g_\parallel = 2.0235$, and $g_\perp = 2.0020$ [45,46]. This large anisotropy implies a strong second-order contribution of the spin-orbit interaction in both the g-tensor and the D-tensor. Indeed, we find only ≈0.7 GHz contribution to the zero-field splitting from the electron spin-electron spin–dipole-dipole interaction (see Ref. [47] for the method) that supports this model. Furthermore, the calculated hyperfine constants (see Ref. [48] for the method) of the ^{61}Ni are smaller ($A_\perp = 25$ MHz; $A_\parallel = 63$ MHz) than those of ^{13}C

TABLE II. Concentration of defects in ppm units as determined from characterization of the sample by PL and FTIR spectroscopy (noted "dark expt.") and by fitting of the photocurrent spectra measured without and with blue illumination (noted "no blue" and "blue," respectively) using *ab initio* calculated ionization cross sections. The concentration of the NiV complex could not be deduced from experiments.

Sample	[NV^-]	[NV^0]	[N_s^0]	[NiV^-]	[NiV^0]
Dark expt.	34	1.1	220 ± 20		
No blue	31.4	1.0	200.0	1.2	0.0
Blue	2.9	29.5	180.0	2.0	0.14

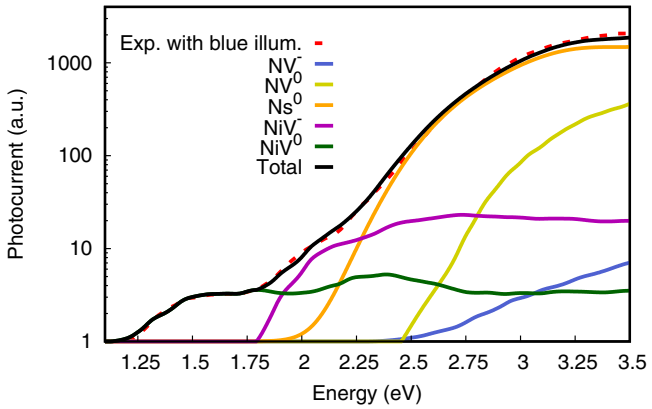

FIG. 3. The photocurrent spectrum measured on our sample under blue illumination (method 2) is fitted to the concentrations of N_s^0, NV^-, NV^0, NiV^-, and NiV^0 defects by using *ab initio* calculated ionization cross sections. The defect concentrations resulting from the fit are listed in Table II, in the line entitled "blue."

($A_\perp = 39$ MHz; $A_\parallel = 84$ MHz) of the six nearest-neighbor C atoms of the Ni atom in diamond, which agrees well with the NOL1/NIRIM5 EPR spectrum (see Fig. 2 in Ref. [46]). This confirms that the NOL1/NIRIM5 EPR center, which is identified as NiV^0, has a stable $S = 1$ spin state at $T = 20$ K temperature [46] and that optically active excited states exist. Similarly to the neutral silicon-vacancy center [49], this defect is thermally stable in boron-doped diamond [46], in agreement with our model. Once the optical spin polarization is confirmed for NiV^0, then our photocurrent spectroscopy measurements show that this center shall be a very promising candidate for photoelectric detection of the spin state operating in the near-infrared region for photoionization.

In conclusion, the presented results show that NiV defect in diamond possesses suitable characteristics to be potentially used as a photoelectrically read solid state qubit operating at room temperature and excited by near-infrared light, presenting interest for quantum information technology. By recording the photocurrent spectra of a diamond sample that contains nitrogen and nickel impurities in the visible and NIR region, we have identified the ∼1.2- and ∼1.9-eV photoionization bands with the single and double acceptor levels of the nickel split-vacancy complex NiV. In Ni-contaminated samples, ionization of the NiV defect contributes therefore to the total photocurrent measured under green illumination used in the PDMR technique to induce two-photon ionization of NV centers. Our *ab initio* calculations enabled us to model precisely the photocurrent spectra and support the conclusions that the NOL1/NIRIM5 EPR center and the 1.22-eV absorption center originate from the $S = 1$ neutral NiV defect. Additionally, a benefit of this work relates to the reduction of the background photocurrent for green laser excitation by identifying the defects in the diamond band gap that lead to achieving a high magnetic resonance contrast.

This work was supported by EU Commission (project DIADEMS with Contract No. 611143). A.G. acknowledges the support from National Research Development and Innovation Office of Hungary within the Quantum Technology National Excellence Program (Project No. 2017-1.2.1-NKP-2017-00001) and QuantERA Q-Magine project (Contract No. 127889). FWO (Flemish Scientific Foundation) Project No. G0E7417N is also acknowledged.

[1] A. M. Zaitsev, *Optical Properties of Diamond* (Springer, Berlin, 2001).
[2] F. Jelezko and J. Wrachtrup, Phys. Status Solidi A **203**, 3207 (2006).
[3] L. Childress, M. V. Gurudev Dutt, J. M. Taylor, A. S. Zibrov, F. Jelezko, J. Wrachtrup, P. R. Hemmer, and M. D. Lukin, Science **314**, 281 (2006).
[4] J. R. Maze, P. L. Stanwix, J. S. Hodges, S. Hong, J. M. Taylor, P. Cappellaro, L. Jiang, M. V. G. Dutt, E. Togan, A. S. Zibrov, A. Yacoby, R. L. Walsworth, and M. D. Lukin, Nature (London) **455**, 644 (2008).
[5] G. Balasubramanian, I. Y. Chan, R. Kolesov, M. Al-Hmoud, J. Tisler, C. Shin, C. Kim, A. Wojcik, P. R. Hemmer, A. Krueger, T. Hanke, A. Leitenstorfer, R. Bratschitsch, F. Jelezko, and J. Wrachtrup, Nature (London) **455**, 648 (2008).
[6] L. Rondin, J.-P. Tetienne, T. Hingant, J.-F. Roch, P. Maletinsky, and V. Jacques, Rep. Prog. Phys. **77**, 056503 (2014).
[7] F. Dolde, M. W. Doherty, J. Michl, I. Jakobi, B. Naydenov, S. Pezzagna, J. Meijer, P. Neumann, F. Jelezko, N. B. Manson, and J. Wrachtrup, Phys. Rev. Lett. **112**, 097603 (2014).
[8] P. Neumann, I. Jakobi, F. Dolde, C. Burk, R. Reuter, G. Waldherr, J. Honert, T. Wolf, A. Brunner, J. H. Shim, D. Suter, H. Sumiya, J. Isoya, and J. Wrachtrup, Nano Lett. **13**, 2738 (2013).
[9] D. M. Toyli, C. F. de las Casas, D. J. Christle, V. V. Dobrovitski, and D. D. Awschalom, Proc. Natl. Acad. Sci. U.S.A. **110**, 8417 (2013).
[10] P. C. Maurer, G. Kucsko, C. Latta, L. Jiang, N. Y. Yao, S. D. Bennett, F. Pastawski, D. Hunger, N. Chisholm, M. Markham, D. J. Twitchen, J. I. Cirac, and M. D. Lukin, Science **336**, 1283 (2012).
[11] W. Pfaff, B. J. Hensen, H. Bernien, S. B. van Dam, M. S. Blok, T. H. Taminiau, M. J. Tiggelman, R. N. Schouten, M. Markham, D. J. Twitchen, and R. Hanson, Science **345**, 532 (2014).
[12] B. Hensen, H. Bernien, A. E. Dréau, A. Reiserer, N. Kalb, M. S. Blok, J. Ruitenberg, R. F. L. Vermeulen, R. N. Schouten, C. Abellán, W. Amaya, V. Pruneri, M. W. Mitchell, M. Markham, D. J. Twitchen, D. Elkouss, S. Wehner, T. H. Taminiau, and R. Hanson, Nature (London) **526**, 682 (2015).
[13] G. Balasubramanian, P. Neumann, D. Twitchen, M. Markham, R. Kolesov, N. Mizuochi, J. Isoya, J. Achard, J. Beck, J. Tissler, V. Jacques, P. R. Hemmer, F. Jelezko, and J. Wrachtrup, Nat. Mater. **8**, 383 (2009).
[14] A. Gruber, A. Dräbenstedt, C. Tietz, L. Fleury, J. Wrachtrup, and C. von Borczyskowski, Science **276**, 2012 (1997).
[15] E. Bourgeois, A. Jarmola, P. Siyushev, M. Gulka, J. Hruby, F. Jelezko, D. Budker, and M. Nesladek, Nat. Commun. **6**, 8577 (2015).

[16] F. M. Hrubesch, G. Braunbeck, M. Stutzmann, F. Reinhard, and M. S. Brandt, Phys. Rev. Lett. **118**, 037601 (2017).
[17] E. Bourgeois, E. Londero, K. Buczak, J. Hruby, M. Gulka, Y. Balasubramaniam, G. Wachter, J. Stursa, K. Dobes, F. Aumayr, M. Trupke, A. Gali, and M. Nesladek, Phys. Rev. B **95**, 041402 (2017).
[18] M. Gulka, E. Bourgeois, J. Hruby, P. Siyushev, G. Wachter, F. Aumayr, P. R. Hemmer, A. Gali, F. Jelezko, M. Trupke, and M. Nesladek, Phys. Rev. Appl. **7**, 044032 (2017).
[19] K. Iakoubovskii and G. J. Adriaenssens, J. Phys.: Condens. Matter **13**, 6015 (2001).
[20] L. Rondin, G. Dantelle, A. Slablab, F. Grosshans, F. Treussart, P. Bergonzo, S. Perruchas, T. Gacoin, M. Chaigneau, H.-C. Chang, V. Jacques, and J.-F. Roch, Phys. Rev. B **82**, 115449 (2010).
[21] T.-L. Wee, Y.-K. Tzeng, C.-C. Han, H.-C. Chang, W. Fann, J.-H. Hsu, K.-M. Chen, and Y.-C. Yu, J. Phys. Chem. A **111**, 9379 (2007).
[22] S. C. Lawson, D. Fisher, D. C. Hunt, and M. E. Newton, J. Phys.: Condens. Matter **10**, 6171 (1998).
[23] A. T. Collins and P. M. Spear, J. Phys. D **15**, L183 (1982).
[24] J. E. Lowther, Phys. Rev. B **51**, 91 (1995).
[25] K. Iakoubovskii, A. Stesmans, B. Nouwen, and G. J. Adriaenssens, Phys. Rev. B **62**, 16587 (2000).
[26] J. P. Goss, P. R. Briddon, R. Jones, and S. Öberg, J. Phys.: Condens. Matter **16**, 4567 (2004).
[27] R. Larico, J. F. Justo, W. V. M. Machado, and L. V. C. Assali, Phys. Rev. B **79**, 115202 (2009).
[28] G. Thiering, E. Londero, and A. Gali, Nanoscale **6**, 12018 (2014).
[29] A. P. Yelisseyev and V. A. Nadolinny, Diamond Relat. Mater. **4**, 177 (1995).
[30] A. Gali, E. Janzén, P. Deák, G. Kresse, and E. Kaxiras, Phys. Rev. Lett. **103**, 186404 (2009).
[31] P. Deák, B. Aradi, T. Frauenheim, E. Janzén, and A. Gali, Phys. Rev. B **81**, 153203 (2010).
[32] J. Heyd, G. E. Scuseria, and M. Ernzerhof, J. Chem. Phys. **118**, 8207 (2003).
[33] A. V. Krukau, O. A. Vydrov, A. F. Izmaylov, and G. E. Scuseria, J. Chem. Phys. **125**, 224106 (2006).
[34] J. P. Perdew, K. Burke, and M. Ernzerhof, Phys. Rev. Lett. **77**, 3865 (1996).
[35] G. Kresse and J. Hafner, Phys. Rev. B **47**, 558 (1993).
[36] G. Kresse and J. Furthmüller, Phys. Rev. B **54**, 11169 (1996).
[37] P. E. Blöchl, Phys. Rev. B **50**, 17953 (1994).
[38] C. Freysoldt, J. Neugebauer, and C. G. Van de Walle, Phys. Rev. Lett. **102**, 016402 (2009).
[39] P. Deák, B. Aradi, M. Kaviani, T. Frauenheim, and A. Gali, Phys. Rev. B **89**, 075203 (2014).
[40] See Supplemental Material at http://link.aps.org/supplemental/10.1103/PhysRevB.97.241202 for details on the ionization energies of the nitrogen-related defects in diamond.
[41] M. Nesladek, L. M. Stals, A. Stesmans, K. Iakoubovskij, G. J. Adriaenssens, J. Rosa, and M. Vaněček, Appl. Phys. Lett. **72**, 3306 (1998).
[42] J. Rosa, M. Vaněček, M. Nesladek, and L. Stals, Diamond Relat. Mater. **8**, 721 (1999).
[43] J. C. Inkson, J. Phys. C **14**, 1093 (1981).
[44] S. C. Lawson, H. Kanda, and M. Sekita, Philos. Mag. B **68**, 39 (1993).
[45] V. A. Nadolinny, J. M. Baker, M. E. Newton, and H. Kanda, Diamond Relat. Mater. **11**, 627 (2002).
[46] K. Iakoubovskii, Phys. Rev. B **70**, 205211 (2004).
[47] V. Ivády, T. Simon, J. R. Maze, I. A. Abrikosov, and A. Gali, Phys. Rev. B **90**, 235205 (2014).
[48] K. Szász, T. Hornos, M. Marsman, and A. Gali, Phys. Rev. B **88**, 075202 (2013).
[49] A. M. Edmonds, M. E. Newton, P. M. Martineau, D. J. Twitchen, and S. D. Williams, Phys. Rev. B **77**, 245205 (2008).